

Partial and total widths of the resonances of the $H^{-} 1S$ two-electron ionization ladder

M. Chrysos, Y. Komninos, Th. Mercouris, and C. A. Nicolaidis

*Theoretical and Physical Chemistry Institute, National Hellenic Research Foundation,
48, Vassileos Constantinou Avenue, Athens 11635, Greece*

(Received 1 March 1990)

We have obtained the partial and total widths for autoionization of the $H^{-} 1S$ two-electron ionization ladder for $n=3-7$, which leads to the Wannier state at $E=0$. The theory starts from first principles by identifying and computing the appropriate localized, correlated wave functions on the real energy axis and then incorporating the effects of the multichannel continuum by solving state-specific, complex-eigenvalue non-Hermitian matrix equations. The outgoing channel-dependent Gamow orbitals are expanded in terms of Slater-type orbitals with coordinate complex scaling. The partial widths are obtained from an equation involving the complex mixing coefficients of the resonance wave function and the corresponding off-diagonal matrix element for each open channel. We find that by far the largest partial width is that which comes from the nearest threshold while within this hydrogenic threshold there is strong mixing of the angular momentum channels and a decay rate distribution which depends on the excitation energy.

I. INTRODUCTION

The first-principles quantum-mechanical treatment of multiply excited states (MES) has been one of the challenging problems of atomic physics. Of special interest are those classes of doubly and triply excited states (DES and TES) whose wave functions exhibit localization on the two-electron Wannier ridge^{1,2} and on a three-electron hyperridge.³ The method of identification and systematic computation of correlated wave functions and properties of such states in terms of combinations of suitably chosen orbitals and N -electron function spaces has been presented in a series of publications from this institute.²⁻⁵ According to this theory, the state of interest has the lowest energy within each intrashell manifold and the corresponding root is optimized in a state-specific manner. Its computational implementation is based on the theory of autoionizing states⁶ which introduced and justified the use of Hartree-Fock (HF) or multiconfigurational HF (MCHF) zeroth-order functions for the treatment of MES in combination with structure-dependent one-electron projection operators.

The class of DES whose wave functions satisfy the Wannier condition $|\mathbf{r}_1|=|\mathbf{r}_2|$, $\theta_{12}=\pi$ as n becomes large, and constitute the two-electron ionization ladder (TEIL), lie in the continua of many channels, into which they autoionize. What are their decay probabilities and how do they distribute themselves over the various thresholds? The present work offers answers to these questions for the first time.

In particular, we have computed the partial and total widths for the $1S$ TEIL multichannel resonances of H^{-} which start just below the hydrogen $n=3$ threshold and go up to the $n=7$ threshold. The calculation of partial widths of these highly excited states has become possible by applying the complex-eigenvalue multichannel theory⁷ to the correlated wave functions of the TEIL states.

Given the hydrogenic thresholds of the open channels

for the H^{-} TEIL states, we have computed two kinds of partial widths. The first is with respect to each hydrogenic threshold with index m , channel mixing included. For example, the H^{-} TEIL state of the $n=4$ manifold decays into the $m=1, 2$, and 3 available hydrogenic thresholds. We have found that the major contribution is due to the nearest one, while there is relatively weak coupling between channels of different thresholds. The second type of partial widths corresponds to each individual angular momentum l_m for each m , with inter- and intrathreshold channel mixing included. For example, for the threshold $m=3$, the available orbital angular momenta which can couple with the free electron to give a $1S$ overall symmetry are s, p , and d . We have found that there is a distribution of rates over the l -channels and strong mixing among l -channels of the same threshold.

II. PREVIOUS RESULTS ON WIDTHS OF DOUBLY EXCITED STATES OF H^{-}

In spite of much theoretical work on DES of H^{-} since the early sixties^{1,8,9} and a variety of experimental observations,^{9,10} information on partial widths of the class of highly excited states connected with the Wannier ridge has not been available until now, due to the formal and computational complexity of the problem. On the other hand, quantitative knowledge in this area would increase substantially the level at which the physics of these states is understood. For example, the total inelastic cross section at the vicinity of a DES is determined almost exclusively by resonant scattering. Therefore it is proportional to the partial widths of the DES with respect to the incident channel. In turn, this partial width is proportional to the normalization of the wave function representing the DES. The latter is provided to a good approximation by WKB wave functions of the Wannier type for energies below the ionization threshold. There have been three proposals regarding this semiclassical

TABLE I. Number of configurations used to describe the function $\Phi + X_{as}$, number of rotated Slater-type functions per channel, and optimum values of the nonlinear parameters of each Slater-type orbital (STO).

n	Configurations	Size of STO basis	α_{opt}	θ_{opt}
3	33	10	0.5	-30°
4	64	10	0.5	-20°
5	85	8	0.5	-30°
6	96	6	0.1	-30°
7	91	4	0.1	-20°

wave function normalization N . Rau¹¹ conjectured an energy dependence of $N^2 \sim E^3 \times E^{0.127}$. From a semiclassical theory for negative energies, Macek and Feagin¹² obtained $N^2 \sim E^{3/2} \times E^{1.127}$. More recently, Komninos's¹³ semiclassical analysis of the TEIL states yielded $N^2 \sim E^3 \times E^{0.127}$, in agreement with Rau. Thus it is important to examine further the energy dependence of the partial widths by a method that is not of the WKB type, i.e., via the use of fully quantum-mechanical calculations of correlated wave functions. Table VIII contains the partial width to the $1s$ channel, obtained by us just for this case from the first-order golden rule formula and a numerical Hartree-Fock scattering orbital. This type of computation is justified by the fact that this partial width is very small and the interthreshold coupling is very weak (see Sec. IV). The results yield an energy dependence E^p , $p = 3.4 \pm 0.2$, which is close to the value 3.127 obtained by Komninos.¹³

On the other hand, the total widths have been computed as part of a series of studies on DES by Ho¹⁴ and by Ho and Callaway¹⁵ using the complex coordinate rotation (CCR) method for resonances below the $n = 6$ threshold and by Morgan, McDowell, and Callaway;¹⁶ Hata, Mor-

gan, and McDowell;¹⁷ and Pathak, Kingston, and Berrington¹⁸ using scattering-type methods for resonances below the $n = 4$ threshold. These investigations aimed at the computation of a large number of resonances and have not isolated the TEIL states. However, following the analysis and computations of Ref. 2, we have identified them as being those corresponding to the lowest energy of each manifold.

III. PRESENT THEORY AND CALCULATIONS

The present calculations were done as follows. The wave function for each 1S TEIL state of H^- is written as

$$\Psi^n(E) = \Psi_0^n + X_{as}^n(E), \quad (1a)$$

$$E_0^n \equiv \langle \Psi_0^n | H | \Psi_0^n \rangle, \quad (1b)$$

where Ψ_0^n represents the localized component and $X_{as}(E)$ the asymptotic one representing the open channels. The subshell cluster expansion of $\Psi^n(E)$ (Ref. 19) leads to the possibility of identifying and computing the partial widths to all orders.⁷

In the present case of the 1S TEIL states, the index n represents the principal quantum numbers of the two electrons, $n_1 = n_2 = n$, which characterize the choice of the configurations comprising the zeroth-order MCHF vector.² The choice of such a zeroth-order vector assures the incorporation, in a self-consistent manner, of a large part of the long-range interelectronic correlation and of angular correlation. Given the fact that for each n the MCHF manifold contains n configurations (e.g., for $n = 4, 4s^2, 4p^2, 4d^2, 4f^2$) and n solutions, the root which corresponds to the TEIL state and which, therefore, is optimized, is that with the lowest energy.^{2,5}

Previous experience with state-specific calculations of a variety of autoionizing states²⁰⁻²² and with TEIL states^{2,5} reveals that, in most cases, MCHF solutions con-

TABLE II. Energies (in a.u. from the double ionization threshold) of the H^- 1S TEIL states $n = 3-9$.

$n = 3$	$n = 4$	$n = 5$	$n = 6$	$n = 7$	$n = 8$	$n = 9$
			Present work			
0.068 63	0.039 48	0.025 59	0.017 91	0.013 25		
			Previous work ^a			
0.069 27	0.039 97	0.025 95	0.018 14	0.013 44	0.010 35	0.008 23
			Others			
0.069 16 ^b	0.039 89 ^b	0.025 92 ^b	0.018 18 ^b	0.013 46 ^b	0.010 36 ^b	0.008 22 ^b
0.069 15 ^c						
	0.039 64 ^d	0.0257 ^d	0.018 00 ^d			
0.069 01 ^e						
0.069 01 ^f	0.039 61 ^f					

^aState-specific theory (SST). The open channels have been projected out. Reference 4.

^bReference 23.

^cReference 24.

^dReference 15.

^eReference 25.

^fReference 18.

TABLE III. Total autoionization widths (in a.u.) of the $H^{-1}S$ TEIL states $n=3-7$. The results correspond to the lowest root of each manifold.

$n=3$	$n=4$	$n=5$	$n=6$	$n=7$
0.001 51	0.000 95	Present work 0.000 71	0.000 48	0.000 36
0.001 51 ^b	0.000 95 ^a	Others 0.000 70 ^a	0.000 46 ^a	
0.001 43 ^c	0.001 10 ^b			

^aReference 15.

^bReference 18.

^cReference 25.

stitute very good descriptions of the high-lying states. Thus, for reasons of economy, in this work we chose

$$\Psi_0^n \approx \Phi_{\text{MCHF}}^n, \quad (2a)$$

$$E_0^n \approx E_{\text{MCHF}}^n, \quad (2b)$$

especially since we aimed at establishing valid trends as a function of n and orbital angular momentum rather than extremely accurate total and partial widths. Nevertheless, we were pleasantly surprised to discover that the results on total widths which follow from the approximation (2) and the method described below are in excellent agreement with those from the very extensive CCR computations of Ho¹⁴ and Ho and Callaway¹⁵ (see Table III).

The asymptotic correlation function is written as a sum of the open-channel functions

$$\begin{aligned} X_{\text{as}}^n(E) &= \sum_m X_{\text{as}}^{l_m}(E) \\ &= \sum_{m, l_m} [\Phi_{\text{ion}}^{l_m}(N-1)g^{l_m}(E)], \end{aligned} \quad (3)$$

where l_m denote the open channel. The exact asymptotic form of $X_{\text{as}}(E)$ on resonance emerges from the formalism of configuration interaction in the continuum.¹⁹

Regarding the computational steps, Ψ_0^n and $\Phi_{\text{ion}}^{l_m}(N-1)$ are computed on the real coordinate axis. For the present study of H^{-} , Ψ_0^n is obtained as Φ_{MCHF}^n and $\Phi_{\text{ion}}^{l_m}$

are the exact hydrogenic functions for each m threshold below the energy E_0^n . The Gamow orbitals $g^{l_m}(E)$ are regularized via coordinate complex scaling. Certain simplifications that involve the diagonal and off-diagonal matrix elements of the complex energy matrix reduce the size of the computations drastically.^{7,19} According to these, only the Gamow orbital is subjected to coordinate rotation and is expressed in terms of a state- and channel-specific Slater basis set with coordinates $\rho = re^{-i\theta}$.

The determination of the total and partial widths is done in two steps. The first is diagonalizing the total complex Hamiltonian matrix containing the matrix elements

$$\begin{aligned} E_{\text{MCHF}}^n, \quad &\langle \Phi_{\text{MCHF}}^n | H | X_{\text{as}}^{l_m} \rangle, \\ &\langle X_{\text{as}}^{l_m} | H | \Phi_{\text{MCHF}}^n \rangle, \quad \langle X_{\text{as}}^{l_m} | H | X_{\text{as}}^{l_m} \rangle, \end{aligned}$$

and the second is searching for the region in the parameter space where the imaginary part of the complex energy is independent of θ .

Having thus optimized the function space, the all-order partial complex eigenvalues are given by⁷

$$z^{l_m} \equiv \delta^{l_m} - \frac{i}{2} \gamma^{l_m} \quad (4a)$$

$$= \frac{C_{l_m}}{C_{\text{MCHF}}^n} \langle \Phi_{\text{MCHF}}^n | H | X_{\text{as}}^{l_m} \rangle, \quad (4b)$$

TABLE IV. Partial autoionization widths (in a.u.) with respect to each group m of open channels. The greatest contribution comes from the nearest group $m = n - 1$. As the level of excitation increases, the interthreshold channel coupling becomes weaker. However, as it can be seen from Table VII, the intrathreshold channel coupling is very strong.

m		$n=3$	$n=4$	$n=5$	$n=6$	$n=7$
$n-1$	γ_{dec}	0.00 154	0.000 95	0.000 67	0.000 43	0.000 31
$n-1$	γ_{coup}	0.00 147	0.000 90	0.000 65	0.000 41	0.000 29
$n-2$	γ_{dec}	0.000 09	0.000 09	0.000 06	0.000 06	0.000 05
$n-2$	γ_{coup}	0.000 04	0.000 06	0.000 06	0.000 06	0.000 05
$n-3$	γ_{dec}		0.000 01	0.000 01	0.000 01	0.000 01
$n-3$	γ_{coup}		0.000 00	0.000 00	0.000 01	0.000 01

where c_{l_m} and C_{MCHF}^n are the mixing coefficients with interchannel coupling, δ^{l_m} is the partial energy shift, and γ^{l_m} is the partial width. The total width of each TEIL state is then the sum of the partial widths

$$\Gamma^n = \sum_m \gamma^m = \sum_m \sum_{l_m} \gamma^{l_m}. \quad (5)$$

IV. RESULTS

Table I contains the technical information pertaining to the calculations. The resulting energies and total widths are given in Tables II and III, respectively. Figure 1 shows how stabilization of the width is established as a function of the number of the available configurations corresponding to each threshold m . Sudden jumps occur as each threshold opens and contributes with new orbital momenta. In the limit, all possible momenta are included and the stabilized eigenvalue yields the total resonance width of the TEIL state.

Table III shows that the lifetime of the TEIL states increases with increasing energy. Furthermore, it is clear from Tables III and IV that the largest contribution by far to the total width comes from the nearest threshold $m = n - 1$. The partial widths of the lower channels are orders of magnitude smaller, the difference caused mainly by the rapidly changing electronic wave functions with consequent changes in the overlap between initial and final states in the region where the mechanism of autoionization occurs.²²

For the TEIL states $n \leq 7$, the closest group of open channels corresponds to the hydrogenic threshold ($n - 1$). However, a drastic change occurs at $n = 8$ (see Fig. 2). The (negative) energy of this state (see Table II)

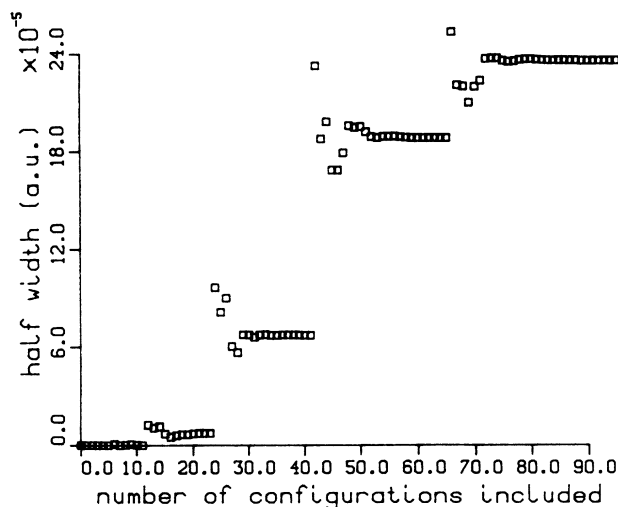


FIG. 1. Plot of the convergence of autoionization half-width (in a.u.) of the $n = 6$ $1S$ TEIL state of H^- , as a function of the number of asymptotic correlation vectors. Each jump represents a stabilized result with respect to the sum of orbital momenta which can couple to the core of the channels below. The final jump includes Gamow orbitals with s , p , d , f , and g angular momenta.

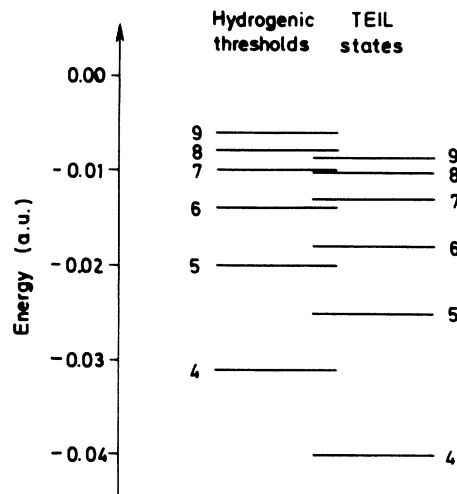


FIG. 2. Energy-level diagram of the $H^- S$ TEIL states ($n = 4-9$). Starting with the state $n = 8$, the energies fall below the hydrogenic thresholds with quantum number $n - 1$.

turns out to be slightly lower than the one corresponding to the hydrogenic threshold with principal quantum number 7. Thus, for TEIL states $n \geq 8$, the channels ($n - 1$) are no longer open, and therefore they start contributing to the localized component of the total wave function. This phenomenon is expected to become more pronounced for higher n , since an increasing number of channels gradually close. It is still an open question, however, whether and to what extent the new closed channels contribute additively to the width of the resonance, which is otherwise expected to decrease rapidly as soon as the most significant open channels close.

In Table IV we present the results from our study of the all-order interchannel coupling. The upper row in Table IV contains the results of computations where there is no coupling among channels of different thresholds. The resulting decoupled partial widths are designated by γ_{dec} . The lower row (γ_{coup}) contains the results with the aforementioned coupling included, as obtained from the diagonalization of the total complex eigenvalue Hamiltonian matrix and Eqs. (4). The conclusion is that the major contribution comes from the nearest threshold and that its contribution is basically unaltered by mixing of channels belonging to different thresholds. This finding justifies the computations of Table V for the $1s$ threshold, which were done with the golden rule and high numerical accuracy in order to obtain reliably very small widths.

Finally, the theory allows the computation and analysis

TABLE V. Partial widths to the $1s$ channel (in a.u.), of the TEIL states $n = 4-7$ of $H^{-1}S$. The results are obtained from the golden rule formula and numerical Hartree-Fock scattering functions.

$n = 4$	$n = 5$	$n = 6$	$n = 7$
1.31×10^{-5}	2.26×10^{-6}	6.58×10^{-7}	2.94×10^{-7}

TABLE VI. Partial-width analysis within the threshold $m = n - 1$. Results are given in a.u. and as a percentage of the total widths of Table III. As the level of excitation increases, the distribution moves towards higher momenta in a manner similar to that of the weights of the bound configurations. Moreover, as it can be seen from the last row, for higher n states the contribution of the lower thresholds becomes more important.

	$n = 3$	$n = 4$	$n = 5$	$n = 6$	$n = 7$
$(n - 1)s\epsilon s$	0.001 12 74.55%	0.000 46 48.44%	0.000 25 36.06%	0.000 13 27.33%	0.000 08 22.90%
$(n - 1)p\epsilon p$	0.000 35 23.12%	0.000 41 42.75%	0.000 32 45.39%	0.000 20 41.31%	0.000 13 36.96%
$(n - 1)d\epsilon d$		0.000 03 2.93%	0.000 07 9.91%	0.000 08 15.92%	0.000 06 17.95%
$(n - 1)f\epsilon f$			0.000 00 0.34%	0.000 00 1.65%	0.000 01 3.60%
$(n - 1)g\epsilon g$				0.000 00 0.01%	0.000 00 0.25%
$\gamma_{\text{coup}} = \sum_l (n - 1)l\epsilon l$	0.001 47 97.67%	0.000 90 94.12%	0.000 65 91.70%	0.000 41 86.22%	0.000 29 81.66%

TABLE VII. Partial-width analysis within the threshold $m = n - 1$, with the intrathreshold channel mixing neglected. The sum of the partial widths exceeds substantially the total width of the state.

	$n = 3$	$n = 4$	$n = 5$	$n = 6$
$(n - 1)s\epsilon s$	0.001 31	0.000 70	0.000 49	0.000 39
$(n - 1)p\epsilon p$	0.000 41	0.000 62	0.000 51	0.000 38
$(n - 1)d\epsilon d$		0.000 06	0.000 12	0.000 17
$(n - 1)f\epsilon f$			0.000 01	0.000 02
$(n - 1)g\epsilon g$				0.000 00
$\gamma_{\text{dec}} = \sum_l (n - 1)l\epsilon l$	0.001 72	0.001 38	0.001 13	0.000 96

TABLE VIII. Percentage of the total width of the partial autoionizing widths of the TEIL state $n = 6$ (in a.u.), with respect to each threshold $m = n - 1$ of open channels. As i increases, the distribution moves towards lower momenta.

$n = 6$	$i = 1$	$i = 2$	$i = 3$	$i = 4$
$(n - i)s\epsilon s$	27.33%	4.43%	0.75%	0.14%
$(n - i)p\epsilon p$	41.31%	6.35%	0.78%	0.03%
$(n - i)d\epsilon d$	15.92%	1.16%	0.01%	
$(n - i)f\epsilon f$	1.65%	0.00%		
$(n - i)g\epsilon g$	0.01%			
$\gamma_{\text{coup}} = \sum_l (n - i)l\epsilon l$	0.000 41 86.22%	0.000 06 11.94%	0.000 01 1.54%	0.000 00 0.17%

of the distribution of decay rates within each threshold m , as a function of the angular momentum l_m . In other words, the dynamics of decay of, say, the $n=3$ 1S TEIL state to the $m=2, l=0, 1$ channels can be determined absolutely. Tables VI and VII contain our results for the decay to the nearest threshold, with and without interchannel mixing, respectively. Two findings are particularly interesting: first, that there is a distribution of probability over the l channels with a clear energy (n) dependence; second, that interchannel mixing is very strong for channels of the same threshold. This is concluded from the fact that the sum of the partial widths of Table VII referring to a given state exceeds by far the total widths of the state. As a last piece of information, Table VIII contains the partial width analysis for the state $n=6$ with respect to all the lower thresholds.

V. SYNOPSIS

We have presented reliable results for the partial and total widths of the class of highly excited 1S resonances in H^- which lead to the Wannier state at threshold.^{1,2} Our approach employed state-specific wave functions with angular and long-range radial correlations²⁻⁶ and accounted for interthreshold as well as intrathreshold channel mixing in the continuous spectrum via the complex-eigenvalue polyelectronic theory.⁷ The established trends for the widths of these resonances are the total width decreases with increasing excitation, the nearest threshold yields the largest partial width by an order of magnitude, and within that hydrogenic threshold there is strong l -channel mixing and a decay rate distribution which is dependent on the excitation energy.

¹U. Fano, Rep. Prog. Phys. **46**, 97 (1983).

²Y. Komninos and C. A. Nicolaides, J. Phys. B **19**, 1701 (1986); C. A. Nicolaides, and Y. Komninos, Phys. Rev. A **35**, 999 (1987).

³Y. Komninos, M. Chrysos, and C. A. Nicolaides, Phys. Rev. A **38**, 3182 (1988); C. A. Nicolaides, M. Chrysos, and Y. Komninos, *ibid.* **41**, 5244 (1990).

⁴Y. Komninos, M. Chrysos, and C. A. Nicolaides, J. Phys. B **20**, L791 (1987).

⁵C. A. Nicolaides, M. Chrysos, and Y. Komninos, J. Phys. B **21**, L73 (1988); Phys. Rev. A **39**, 1523 (1989).

⁶C. A. Nicolaides, Phys. Rev. A **6**, 2078 (1972).

⁷C. A. Nicolaides and D. R. Beck, Phys. Lett. **65A**, 11 (1978); Int. J. Quantum Chem. **14**, 457 (1978); C. A. Nicolaides and Th. Mercouris, Phys. Rev. A **32**, 3247 (1985); **36**, 390 (1987).

⁸T. F. O'Malley and S. Geltman, Phys. Rev. **137**, A1344 (1965); A. Temkin and J. F. Walker, *ibid.* **140**, A1520 (1965).

⁹J. S. Risley, in *Atomic Physics 6*, edited by R. J. Damburg (Plenum, New York, 1979), p. 223.

¹⁰H. C. Bryant, B. D. Dieterle, J. Donohue, H. Sharifian, H. Tootoonchi, D. M. Wolfe, P. A. M. Gram, and M. A. Yates-Williams, Phys. Rev. Lett. **38**, 228 (1977); C. Y. Tang, P. G. Harris, A. H. Mohagheghi, H. C. Bryant, C. R. Quick, J. B. Donahue, R. A. Reeder, S. Cohen, W. W. Smith, and J. E. Stewart, Phys. Rev. A **39**, 6068 (1989).

¹¹A. R. P. Rau, in *Atomic Physics 9*, edited by R. S. van Dyck and E. N. Fortson (World Scientific, Singapore, 1984), p. 491.

¹²J. Macek and J. M. Feagin, J. Phys. B **18**, 2161 (1985).

¹³Y. Komninos (unpublished).

¹⁴Y. K. Ho, J. Phys. B **10**, L373 (1977); **12**, L543 (1979).

¹⁵Y. K. Ho and J. Callaway, Phys. Rev. A **34**, 130 (1986).

¹⁶L. A. Morgan, M. R. C. McDowell, and J. Callaway, J. Phys. B **10**, 3297 (1977).

¹⁷J. Hata, L. A. Morgan, and M. R. D. McDowell, J. Phys. B **13**, 4453 (1980).

¹⁸A. Pathak, A. E. Kingston, and K. A. Berrington, J. Phys. B **21**, 2939 (1988).

¹⁹C. A. Nicolaides, Y. Komninos, and Th. Mercouris, Int. J. Quantum Chem. Symp. **15**, 355 (1981).

²⁰Y. Komninos, G. Aspromallis, and C. A. Nicolaides, Phys. Rev. A **27**, 1865 (1983).

²¹G. Aspromallis, Y. Komninos, and C. A. Nicolaides, J. Phys. B **17**, L151 (1984).

²²Y. Komninos, N. Makri, and C. A. Nicolaides, Z. Phys. D **2**, 105 (1986); C. A. Nicolaides, N. Makri, and Y. Komninos, J. Phys. B **19**, 1701 (1987).

²³J. M. Rost and J. S. Briggs, J. Phys. B **22**, 3587 (1989).

²⁴L. Lipsky, R. Anania, and R. M. Connelly, At. Data Nucl. Data Tables **20**, 127 (1977).

²⁵J. Callaway, Phys. Rev. A **26**, 199 (1982).